2-1-2008

Biotemplated synthesis of metallic nanoparticle chains on an alpha-synuclein fiber scaffold

Robert Colby
Purdue University, rcolby@purdue.edu

J Hulleman
Department of Medicinal Chemistry and Molecular Pharmacology, Purdue University, jhullema@purdue.edu

Sonal Padalkar
spadalka@purdue.edu

J C. Rochet
Department of Medicinal Chemistry and Molecular Pharmacology, Purdue University, jrochet@purdue.edu

L Stanciu
Birck Nanotechnology Center and School of Materials Engineering, Purdue University, lstanciu@purdue.edu

Journal of
Nanoscience and Nanotechnology
Vol. 8, 973–978, 2008

Biotemplated Synthesis of Metallic Nanoparticle Chains on an α-Synuclein Fiber Scaffold

R. Colby[1,2], J. Hulleman[3], S. Padalkar[1,2], J. C. Rochet[3], and L. A. Stanciu[1,2,*]

[1] *School of Materials Engineering, Purdue University, West Lafayette, Indiana 47907, USA*
[2] *Birck Nanotechnology Center, Purdue University, West Lafayette, Indiana 47906, USA*
[3] *Department of Medicinal Chemistry and Molecular Pharmacology, Purdue University, West Lafayette, Indiana 47907, USA*

Biomolecular templates provide an excellent potential tool for bottom-up device fabrication. Self-assembling α-synuclein protein fibrils, the formation of which has been linked to Parkinson's disease, have yet to be explored for potential device fabrication. In this paper, α-synuclein fibrils were used as a template for palladium (Pd), gold (Au) and copper (Cu) nanoparticle chains synthesis. Deposition over a range of conditions resulted in metal-coated fibers with reproducible average diameters between 50 and 200 nm. Active elemental palladium deposited on the protein fibrils is used as a catalyst for the electroless deposition of Au and Cu. Nanoparticle chains were characterized by scanning electron microscopy (SEM), transmission electron microscopy (TEM), X-ray energy dispersive spectrometry (XEDS), and electron energy loss spectrometry (EELS).

Keywords: Nanowires, Nanoparticles, Amyloid, Electroless Deposition.

1. INTRODUCTION

A major goal in the field of nanotechnology is bottom-up device fabrication using self-assembling materials. Biomolecular templates have the potential to meet the challenge. DNA,[1,2] viruses,[3] and other self-assembling peptide-based structures[4] provide a natively nanoscale template for the fabrication of particles, fibers, and tubes. Biomolecular templates have been successfully used to create conducting,[5] semiconducting,[6] and magnetic structures.[7] Peptide recognition and biologically engineered functionalities have been exploited to fabricate simple self-organizing networks[8] and might eventually be used to design entire self-assembling circuits. Furthermore, biologically-based fabrication schemes can usually be designed to work at room temperature and pressure, and have been successfully implemented alongside traditional circuit fabrication techniques, such as photolithography.

A great amount of effort has been invested in the metallization of biomolecular templates over the past decade. Ever since the first successful results for metallized DNA were published by Braun,[5] a number of templates and coatings have been explored. In addition to the continued study of DNA, research has been conducted on amyloid peptides[9] and viruses, foremost among them tobacco mosaic virus (TMV) and M13 bacteriophage.[10,11] DNA offers the simplest potential for biological encoding, and is not very rigid. Most successful DNA metallization, including silver, gold, palladium, platinum, copper, and cobalt metallization, at least partly as a result of DNA's relative flimsiness, have been particularly irregular in appearance when continuously coated.[1,2] In addition to minerals, DNA has been similarly coated with conducting polyaniline.[12]

Amyloid proteins are more rigid than DNA, but not as straightforward to "program." However, many successful attempts have demonstrated limited success with self-organizing three-way junctions, and matching antibody outer coatings to self-assembled monolayers (SAMs) for directing nanowire deposition on a substrate.[1,2] Furthermore, while DNA may be more directly programmable, peptide polymers surfaces can be modified to accept, for instance, metal ions.[13,14] Polypeptides can also be designed to self-assemble in a number of morphological configurations, including strands, helices, and coaxial tubes. In a study by Carny et al.,[15] coaxial Ag/Au nanofibers were patterned onto a base peptide self-assembled from diphenylalanine. Customizable control of template morphology could allow for a wide range of clever applications and devices.

Viruses, on the other hand are produced with extremely regular dimensions and morphology. TMV, for instance, can be used as a measurement standard for transmission electron microscopy (TEM). TMV has both an inner and outer channel, each with a distinct affinity. Metallized

*Author to whom correspondence should be addressed.

TMV will often assemble end to end.[10] Under the correct conditions, metallized M13 bacteriophage will organize into a liquid crystal when deposited on a surface.[11]

Alpha-synuclein is a 140 amino acid protein that is abundant in mammalian brains, including those of humans. The role of α-synuclein is, as yet, not well understood.[16] However, in humans, the organization of α-synuclein into fibrils has been linked to the onset of Parkinson's disease.[17] Three point mutations of α-synuclein which encourage self-assembly have been discovered; A53T, A30P, and E46K. E46K, a α-synuclein mutant in which the forty-sixth residue is lysine (K) instead of glutamate (E), was used in this study. The fibrillization mechanism for α-synuclein is complex and involves the formation of protofibrils, consisting of annular, spherical, tubular, stacked sheets, and helical morphologies. It is expected that much of the variation in observed morphologies lies in the methodology, as many of the studies used atomic force microscopy of the sub-5 nm protofibrillar structures, dried on a flat surface (mica or similar). The fibrillar morphology of α-synuclein has been inspected by TEM after negative staining with uranyl acetate.[18]

2. EXPERIMENTAL DETAILS

2.1. Materials

α-Synuclein fibrils (E46K) were self-assembled following a procedure described elsewhere.[19] Briefly, purified, lyophilized α-synuclein was dissolved in phosphate-buffered saline (PBS, pH 7.4) with 0.02% (w/v) NaN_3. Filtration through a 0.22 nylon spin filter, followed by a Microcon-100 spin filter yielded a stock solution that was depleted of aggregates. The filtered solution was then dialyzed against the PBS/NaN_3 buffer for 24 hours at 4 °C. The α-synuclein was allowed to self-assemble into fibers by diluting the stock solution with PBS/NaN_3 to a total protein concentration of 100–300 μM (determined by a BCA assay). The solution was incubated in a slowly rotating wheel at 37 °C for 12–96 hours. The fibrillar morphology of the incubated proteins was confirmed by TEM imaging of samples stained with a 2% uranyl acetate solution (Fig. 1). Fibrils incubated for 96 hours were used for metallization experiments (with the exception of a few control groups). The provided solutions, as described above, were further diluted to 1 μM concentration in PBS buffer before further use.

The DMAB reduction solution was prepared by dissolving 62.5 mg of solid DMAB in 25 mL of deionized water (∼0.04 M). The solution was stirred for several hours and filtered through a Whatman® No. 42 filter paper. The base pH of this stock solution was approximately 7.2. Nitric acid or citric acid was used to create acidic reduction solutions with pH between 7.2 and 5.4. Ammonium hydroxide or sodium hydroxide was used to create basic DMAB solutions ranging between a pH of 7.2 and 8.1.

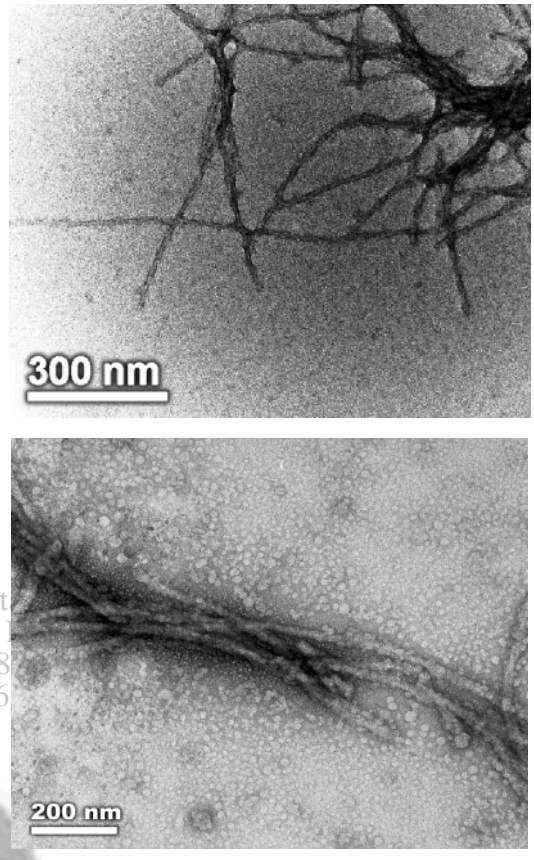

Fig. 1. TEM images of α-synuclein stained with a 1% uranyl acetate solution revealing an average diameter of less than 10 nm. (a) Positively stained regions suggest a helical structure. (b) Fibers were often found loosely grouped together into bundles.

The Pd^{2+} solution was created by dissolving 200 mg of $Pd(CH_3COO)_2$ (palladium acetate) in 25 mL deionized water by stirring for several hours and then filtering through a funnel. This process was repeated twice to make sure the salt was dissolved.

The Cu^{2+} solution contained 446 mg of copper (II) chloride in 25 mL of deionized water was subjected to reduction to DMAB. A gold (Au^{2+}) solution was also produced using gold (II) chloride in 25 mL of deionized water by following a similar protocol. All solutions were individually stored in small quantities and mixed before use by repeatedly withdrawing and expelling the solution with a micropipette. Solutions were often additionally mixed in an ultrasonic bath for approximately 5 minutes before use.

Nanoparticle chains were synthesized both on silicon wafers and on TEM grids. The silicon wafers contained a naturally forming SiO_2 layer on the surface, confirmed by attempted resistance measurements with a digital multimeter (no conducting contact could be established). Most of the TEM grids used contained a thin (approximately 100 nm) layer of amorphous carbon supported by a 3 mm-diameter, 400 mesh grid of copper. Variations used in these experiments include holey carbon grids, wherein

the carbon layer contains regularly spaced holes with a diameter on the order of a micron; amorphous silica grids (100 mesh), in which a thin silica sheet replaces the standard carbon; and gold support grids, for which the support grid is gold instead of copper.

2.2. Synthesis of Pd Nanoparticle Chains

α-Synuclein was deposited onto a substrate with a micropipetter, and then dried in a desiccator. The distribution of the α-synuclein fibrils was found to be improved by depositing the droplet onto a clean wax surface, transferring the droplet to the grid by touching the coated side of the grid to the droplet, and gently lifting. This is a common technique which takes advantage of the natural tendency for small hydrophobic entities to migrate to the air interface of a droplet. Most TEM samples were prepared using this approach. For TEM grid samples, 6 μL of α-synuclein was generally deposited in this manner. A larger, 25 μL volume of solution was typically deposited on silicon wafer samples (silicon wafers were prepared with a much larger surface than the TEM grids). Pd nanoparticle chains were synthesized on α-synuclein fiber scaffolds starting from a 1:10 dilution of the stock α-synuclein fibers deposited on a silicon wafer. Then, $Pd(CH_3COO)_2$ was added and incubated for 5 minutes, followed by 5 minutes reduction with DMAB Best results were obtained for palladium-exposed TEM samples prepared by depositing 5 μL of the palladium solution (diluted as desired) on a α-synuclein loaded grid. After five minutes, 1 μL of the DMAB reduction solution, with the pH adjusted to a value of 7.6, was added directly to the droplet of palladium solution. After another five minutes, the grid was rinsed in deionized water and dried with forced gas. For SEM samples, larger volumes of both the metal salt and reduction solution were used to match the larger volume of fibril solution deposited, while maintaining a 5:1 volume ratio of metal to DMAB. While the above combination yielded the most apparently favorable samples, the process was also tested with reduction times between 30 seconds and 30 minutes, across the full range of DMAB pH values.

2.3. Synthesis of Cu and Au Nanoparticle Chains

Cu and Au nanoparticle chains were fabricated by a two step process requiring palladium as a catalyst. For each metal, 5 μL of the palladium solution was first deposited on the substrate and allowed to dry completely in a desiccator. Then, 5 μL of the desired metal salt solution (copper or gold chloride) was deposited on the substrate and allowed to react with the aminoacyl side chains of the protein for approximately 10 minutes. Lastly, 1 μL of a DMAB solution was added to the metal solution droplet, and allowed to react a further five minutes before being rinsed in deionized water and dried with forced gas. The pH of the DMAB solution was typically between 7.2–7.8.

2.4. Electron Microscopy Characterization

All SEM analysis was performed on a Hitachi S4800 field emission microscope. TEM imaging was performed on a JEOL 2000FX operating at 200 kV, acquired with a side-mounted 1 k CCD camera, or a Philips CM-10 operating at 100 kV (images acquired on Kodak Electron Image Film type S0-163). TEM images were taken with features of interest at moderate defocus, as is typical of similar work in the field. It should be noted that many of the samples are taken at significant defocus to reduce the apparent distortion caused by the nontrivial height variation of the imaged samples. Images used for feature-size measurements were taken near focus where possible. Diffraction patterns were taken on the JEOL 2000FX operating with a eucentric objective lens current of calibrated at approximately 7.035 A. Electron energy loss spectroscopy (EELS) was acquired on an FEI Titan 80/300 TEM equipped with a Gatan Imaging Filter (GIF) and a 2 k CCD, operating at 300 kV. The imaging filter was also used to acquire energy filtered TEM (EFTEM) images. Elemental maps were acquired using a 10 eV slit width. X-ray energy dispersive spectroscopy (XEDS) was performed on a Tecnai F20ST with an EDAX detector (super ultra thin window, 30 mm^2). A beryllium holder was used when acquiring all XEDS data. To determine the sample composition, XEDS data was acquired with the beam focused to a point on the sample, and each acquisition was paired with a reference acquisition from a nearby empty section of TEM grid.

3. RESULTS AND DISCUSSION

In the simplest electroless chemical reduction bath systems, the tunable factors for controlling metal deposition rate are bath pH, reduction time, and reactive salt concentrations.[20] The system to be examined is a small closed system in which it is reasonable to treat the effects of pH, reduction time, and concentrations independently.

Pd nanoparticle chains are of particular interest as electroless deposition of elemental Cu and Au require active Pd as a catalyst.

3.1. Palladium Nanoparticle Chains

The synthesis procedure described above resulted in nanoparticle chains with an average diameter of 90 nm. The nanostructures appeared continuous over several microns. Backscattered electron imaging of the samples in the SEM confirmed that they were conducting (i.e., metallic). Figure 2 shows an SEM image of a Pd nanoparticle chain, prepared on a silicon wafer, at a pH of 7.6. Variations in the reduction time did not lead to modifications in nanoparticle diameter.

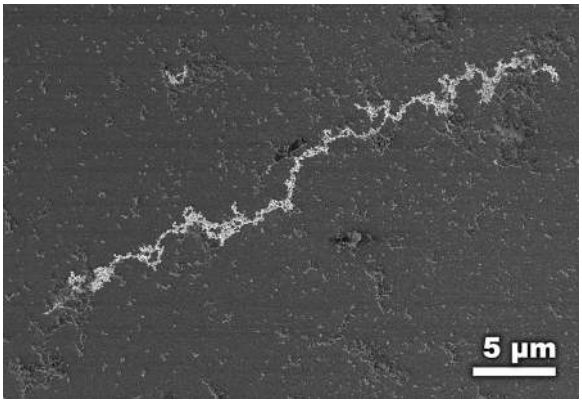

Fig. 2. SEM image of a Pd sample prepared on silicon wafer at a pH of 7.6.

3.2. Transmission Electron Microscopy (TEM) of Pd Nanoparticle Chains

Samples fabricated with a 5 minute reduction at pH= 7.2 were reproduced on carbon coated copper grids for TEM analysis. The synthesis resulted in clearly distinguishable metallic nanoparticle chains (Fig. 3). Attempted diffraction suggested that particles were amorphous. The average diameter of the nanoparticle chains was observed to be of 110 nm (Fig. 3). A reduction in the palladium salt concentration to 0.1 mM, led to the formation of thinner nanoparticle chains, with an average diameter of 50 nm (Fig. 4).

3.3. Gold Nanoparticle Chains

Gold samples were produced under Pd catalysis, by the general procedure described above (0.1 mM). The average diameter of the nanoparticles was about 100 nm. EELS was used to confirm nanoparticle composition. However, EELS confirmation of gold is complicated by the absence of observable edges; only the M(IV), M(V) edges, at

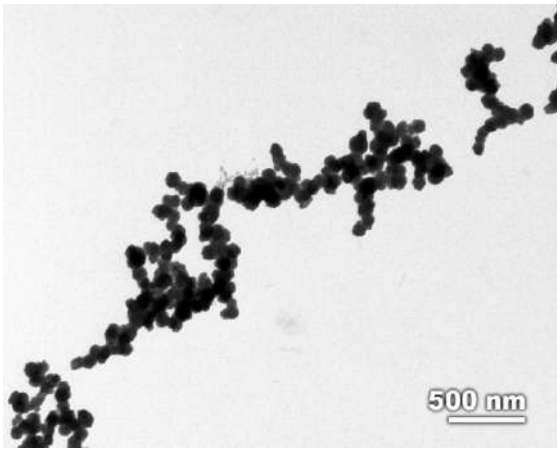

Fig. 3. TEM image of typical Pd nanoparticle chains prepared on TEM grids, from a $Pd(CH_3COO)_2$ solution of 0.3 M concentration.

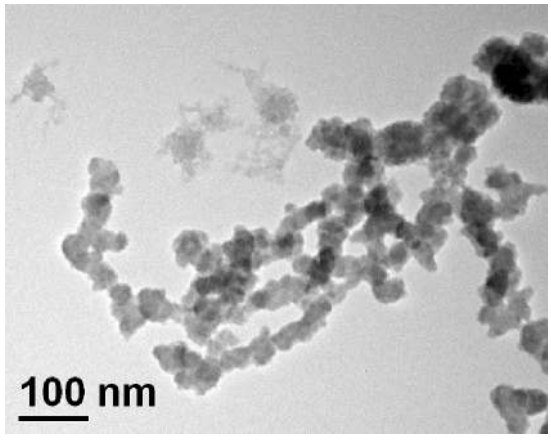

Fig. 4. TEM images of typical samples prepared on TEM grids, 0.1 mM concentration of $Pd(CH_3COO)_2$ solution.

2291 eV and 2206 eV, are expected to be visible with EELS. As it has been noted, the resolution of the instrumentation tends to fall off in the range of 2000 eV, making observations of gold difficult. However, a confirmed EELS measurement of a gold sample was obtained (Fig. 5). As a result of the small signal to noise ratio in the range of the salient M-edge readings, subtracting the background signal resulted in some negative electron counts, and this

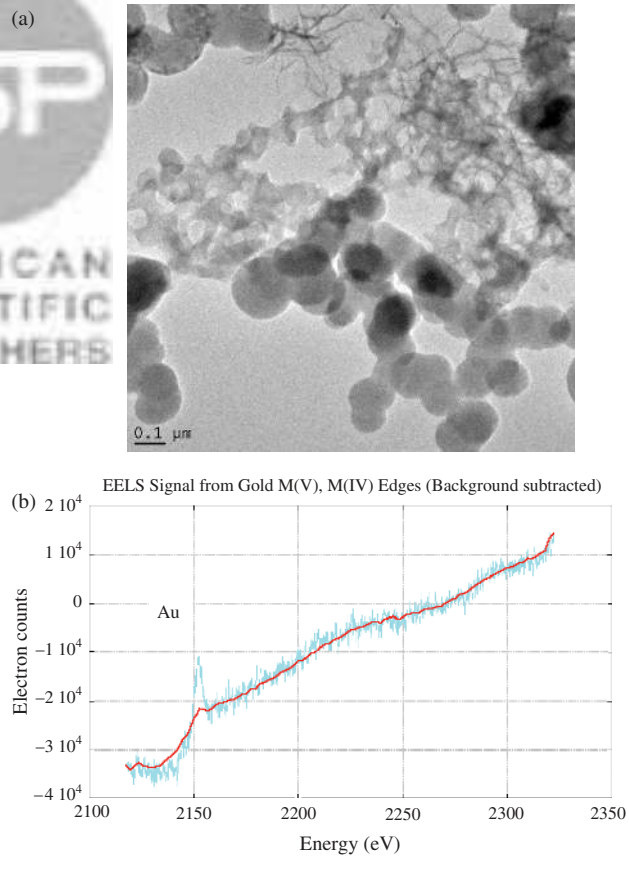

Fig. 5. TEM image of a region of a gold-exposed sample (a) imaged in the FEI Titan and (b) EELS of the region containing the gold M(V), (IV) edges (2206, 2291 eV).

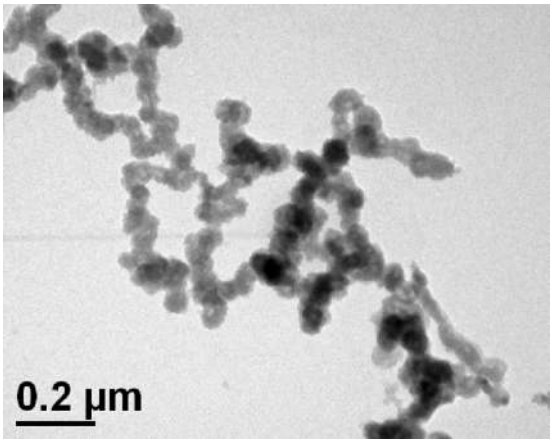

Fig. 6. TEM image of typical Cu nanoparticle chains obtained at pH 7.8.

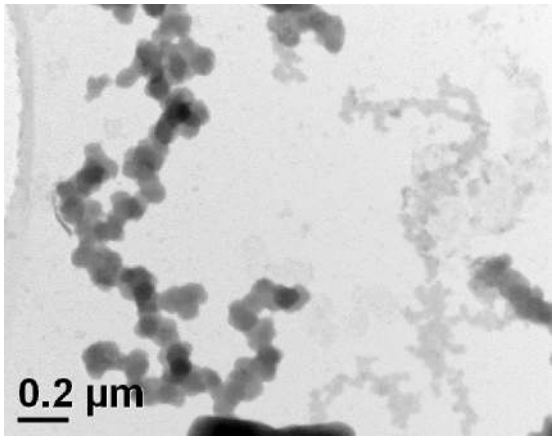

Fig. 8. Representative TEM image of Cu nanoparticle chains obtained by galvanic replacement with gold.

is valid. The problem was further exacerbated by artifacts of previous peaks exposed on the CCD; always an issue, but all the more so in the absence of a strong signal from the sample. Nevertheless, the M(V) edge, in the very least, was indisputably evident.

3.4. Copper Nanoparticle Chains

Samples were fabricated under Pd catalysis, by the general procedure described above. All TEM samples were prepared on gold TEM grids to insure that any copper observed could only have originated from the added salt solution. Initial samples were prepared with a 10 minute exposure to copper chloride and a 5 minute reduction and at a 7.8 pH. Figure 6 shows the synthesized nanoparticle chains with an average diameter of 90 nm.

EELS was used to confirm the presence of Cu. Clear copper L-edges were observed, with distinct white lines indicating the presence of copper oxides (Fig. 7).

Merril reported the reduction of ionic silver to a metallic form in the presence of proteins and DNA.[21, 22] The method is based on the differences between the redox potentials of the biomolecules and those of the matrix and is currently applied for the detection of proteins and nuclein acids. A similar chemical mechanism, in which the metal ions are catalytically reduced to a metallic form in the presence of biomolecules acts during the synthesis of Pd, Cu and Au nanoparticle chains on α-synuclein fiber scaffold. During the metallization process, the cations react with the negatively charged aminoacyl side chains of the protein, at basic pH. In the case of Au and Cu nanoparticle chains, the Pd seeds initially form on the biotemplate and subsequently act as catalysts for Au and Cu deposition.

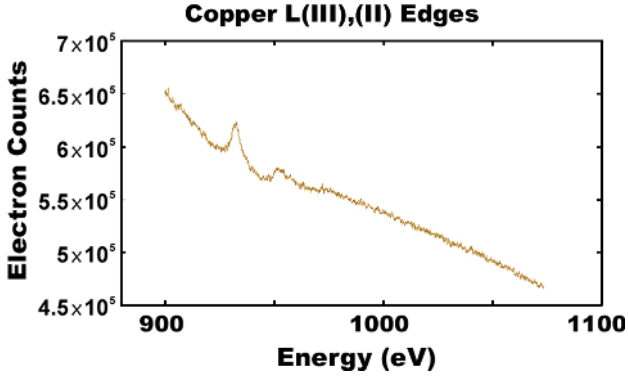

Fig. 7. EELS analysis of Cu nanoparticle chains showing a Cu signal.

3.5. Formation of Cu Nanoparticle Chains by Galvanic Replacement

When Au and Pd nanoparticle chains were first attempted to be synthesized on copper TEM grids, XEDS analysis (Fig. 9) surprisingly showed that the procedure led to the formation of Cu nanoparticle chains instead, by a mechanism called galvanic metal replacement.[23, 24]

Since the standard reduction potential of Cu^{2+}/Cu (0.34 V vs. standard hydrogen electrode, SHE) is smaller than that of Au^{3+}/Au (1.50 V), when Au^{3+} meets Cu from the TEM grid, Cu has the tendency to oxidize to Cu^{2+} and Au^{3+} to reduce to elemental Au. Therefore, instead

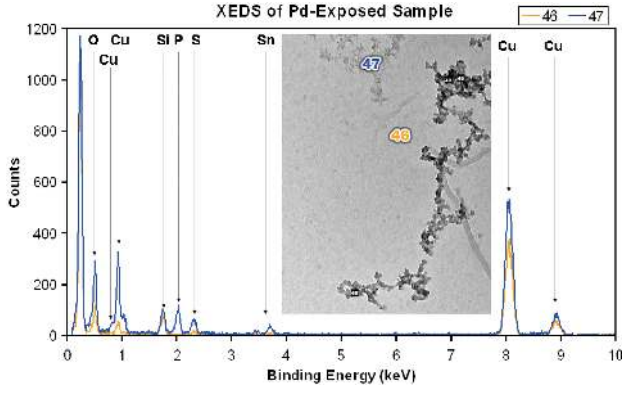

Fig. 9. XEDS of Cu nanoparticle chains obtained by galvanic replacement. Inset image taken on an FEI Tecnai F20ST.

of Au^{3+} ions interacting with negatively charged aminoacyl side chains of α-synuclein fibers, the newly available Cu^{2+} attach to these negatively charged groups and are subsequently reduced to elemental Cu nanoparticles on the surface of the protein, forming nanoparticle chains. Similar results were obtained in the presence of Pd^{2+} and Co^{2+} metal salts, both with standard reduction potentials larger than that of Cu^{2+}/Cu. Figure 8 shows a representative TEM image of Cu nanoparticle chains obtained by galvanic replacement with gold. The diameter of the Cu particles is of about 100 nm.

4. CONCLUSIONS

For the first time, the α-synuclein protein fibrils were used for biotemplated synthesis of Pd, Au and Cu ordered nanoparticle chains. Palladium catalysis is required for the synthesis of Au and Cu ordered nanoparticle chains. Exposing Pd and Au solutions to elemental Cu, in the presence of α-synuclein protein fibers and a reducing agent leads to formation of Cu nanoparticle chains. The results can be expanded to designing bottom-up strategies for nanomaterials synthesis by bio-templated synthesis of other peptides and proteins with the capacity to self-assemble into fibrillar structures with exposed negatively charged groups. These nanostructures have potential applications in nanophotonic devices, ultrahigh-density storage media, or quantum dot arrays.

References and Notes

1. Q. Gu, C. Cheng, and D. T. Haynie, *Nanotechnology* 17, R14 (**2005**).
2. Q. Gu, C. Cheng, R. Gonela, S. Suryanarayanan, S. Anabathula, K. Dai, and D. T. Haynie, *Nanotechnology* 18, R14 (**2006**).
3. C. E. Flynn, S. W. Lee, B. R. Peelle, and A. M. Belcher, *Acta Mater.* 51, 5867 (**2003**).
4. X. Gao and H. Matsui, *Adv. Mater.* 17, 2037 (**2005**).
5. E. Braun, Y. Eichen, U. Sivan, and G. Ben-Yoseph, *Nature* 391, 775 (**1998**).
6. C. Mao, D. J. Solis, B. D. Reiss, S. T. Kottmann, R. Y. Sweeney, A. Hayhurst, G. Georgiou, B. Iverson, and A. M. Belcher, *Science* 303, 213 (**2004**).
7. J. L. Liu, S. Tong, and K. L. Wang, Handbook of Semiconductor Nanostructures and Nanodevices, edited by A. A. Balandin and K. L. Wang, American Scientific Publishers, Los Angeles (**2006**), Vol. 1, p. 1.
8. H. Yan, S. H. Park, Sung Ha, G. Finkelstein, J. H. Reif, T. H. LaBean, and H. Thomas, *Science* 301, 1882 (**2003**).
9. D. Hamada, I. Yanagihara, and K. Tsumoto, *Trends Biotechnol.* 22, 93 (**2004**).
10. W. L. Liu, K. Alim, A. A. Balandin, D. M. Mathews, and J. A. Dodds, *Appl. Phys. Lett.* 86, 1 (**2005**).
11. S. W. Lee, C. Mao, C. E. Flynn, and A. M. Belcher, *Science* 296, 892 (**2002**).
12. P. Nickels, W. U. Dittmer, S. Beyer, J. P. Kotthaus, and F. C. Simmel, *Nanotechnology* 15, 1524 (**2004**).
13. I. A. Banerjee, L. Yu, and H. Matsui, *Proc. Nat. Acad. Sci. USA* 100, 14678 (**2003**).
14. L. Yu, I. A. Banerjee, and H. Matsui, *J. Am. Chem. Soc.* 125, 14837 (**2003**).
15. O. Carny, D. E. Shalev, and E. Gazit, *Nano Lett.* 6, 1594 (**2006**).
16. C. B. Lucking and A. Brice, *Cellular and Molecular Life Sciences* 57, 1894 (**2000**).
17. K. A. Conway, J. D. Harper, and P. T. Lansbury, *Nature Medicine* 4, 1318 (**1998**).
18. V. N. Uversky, J. Li, A. L. Fink, and L. Anthony, *J. Biolo. Chem.* 276, 44284 (**2001**).
19. J. C. Rochet, K. A. Conway, and P. T. Lansbury, *Biochemistry* 39, 10619 (**2000**).
20. G. O. Mallory and J. B. Hajdu, Electroless Plating Fundamentals and Applications, American Electroplaters and Surface Finishers Society, Orlando, Florida (**1990**), p. 1.
21. C. R. Merril, L. Miriam, M. L. Dunau, and D. Goldman, *Anal. Biochem.* 110, 201 (**1981**).
22. C. R. Merril, *Nature* 343, 779 (**1990**).
23. Y. Sun and Y. Xia, *J. Am. Chem. Soc.* 126, 3892 (**2004**).
24. J. Chen, B. Wiley, J. McLellan, Y. Xiong, Z. Y. Li, and Y. Xia, *Nano Lett.* 5, 2058 (**2005**).

Received: 18 January 2007. Accepted: 13 June 2007.